doi:10.1093/brain/awv049 BRAIN 2015: 138; 1410–1423 | 1410

BRAIN
A JOURNAL OF NEUROLOGY

Auditory mismatch impairments are characterized by core neural dysfunctions in schizophrenia

Arnim Johannes Gaebler,[1,2,*] Klaus Mathiak,[1,2,*] Jan Willem Koten Jr.,[3,4] Andrea Anna König,[1,2] Yury Koush,[5,6] David Weyer,[7] Conny Depner,[8] Simeon Matentzoglu,[8] James Christopher Edgar,[9] Klaus Willmes[3] and Mikhail Zvyagintsev[1,2,7]

*These authors contributed equally to this work.

Major theories on the neural basis of schizophrenic core symptoms highlight aberrant salience network activity (insula and anterior cingulate cortex), prefrontal hypoactivation, sensory processing deficits as well as an impaired connectivity between temporal and prefrontal cortices. The mismatch negativity is a potential biomarker of schizophrenia and its reduction might be a consequence of each of these mechanisms. In contrast to the previous electroencephalographic studies, functional magnetic resonance imaging may disentangle the involved brain networks at high spatial resolution and determine contributions from localized brain responses and functional connectivity to the schizophrenic impairments. Twenty-four patients and 24 matched control subjects underwent functional magnetic resonance imaging during an optimized auditory mismatch task. Haemodynamic responses and functional connectivity were compared between groups. These data sets further entered a diagnostic classification analysis to assess impairments on the individual patient level. In the control group, mismatch responses were detected in the auditory cortex, prefrontal cortex and the salience network (insula and anterior cingulate cortex). Furthermore, mismatch processing was associated with a deactivation of the visual system and the dorsal attention network indicating a shift of resources from the visual to the auditory domain. The patients exhibited reduced activation in all of the respective systems (right auditory cortex, prefrontal cortex, and the salience network) as well as reduced deactivation of the visual system and the dorsal attention network. Group differences were most prominent in the anterior cingulate cortex and adjacent prefrontal areas. The latter regions also exhibited a reduced functional connectivity with the auditory cortex in the patients. In the classification analysis, haemodynamic responses yielded a maximal accuracy of 83% based on four features; functional connectivity data performed similarly or worse for up to about 10 features. However, connectivity data yielded a better performance when including more than 10 features yielding up to 90% accuracy. Among others, the most discriminating features represented functional connections between the auditory cortex and the anterior cingulate cortex as well as adjacent prefrontal areas. Auditory mismatch impairments incorporate major neural dysfunctions in schizophrenia. Our data suggest synergistic effects of sensory processing deficits, aberrant salience attribution, prefrontal hypoactivation as well as a disrupted connectivity between temporal and prefrontal cortices. These deficits are associated with subsequent disturbances in modality-specific resource allocation. Capturing different schizophrenic core dysfunctions, functional magnetic resonance imaging during this optimized mismatch paradigm reveals processing impairments on the individual patient level, rendering it a potential biomarker of schizophrenia.

1 Department of Psychiatry, Psychotherapy and Psychosomatics, Medical School, RWTH Aachen University, Aachen, Germany
2 JARA–Translational Brain Medicine, Aachen, Germany
3 Neuropsychology Section, Department of Neurology, Medical School, RWTH Aachen University, Aachen, Germany
4 Neuropsychology Section, Department of Psychology, Karl Franzens University, Graz, Austria
5 Department of Radiology and Medical Informatics, University of Geneva, Geneva, Switzerland

Received July 10, 2014. Revised January 7, 2015. Accepted January 12, 2015. Advance Access publication March 5, 2015

6 Institute of Bioengineering, Ecole Polytechnique Fédérale de Lausanne (EPFL), Lausanne, Switzerland
7 Brain Imaging Facility, IZKF Aachen, RWTH Aachen University, Aachen, Germany
8 Katharina Kasper Via Nobis GmbH, Hospital for Psychiatry and Psychotherapy, Gangelt, Germany
9 Department of Radiology, Lurie Family Foundation MEG Imaging Centre, The Children's Hospital of Philadelphia, Philadelphia, PA, USA

Correspondence to: Arnim Johannes Gaebler,
Department for Psychiatry,
Psychotherapy and Psychosomatics,
RWTH Aachen University,
Pauwelsstr. 30,
52074 Aachen, Germany
E-mail: agaebler@ukaachen.de

Keywords: schizophrenia; functional magnetic resonance imaging; mismatch negativity; classification; multivariate pattern analysis

Abbreviations: ACC = anterior cingulate cortex; GLM = general linear model; MEG = magnetoencephalography; MMN = mismatch negativity; NMDAR = *N*-methyl D-aspartate receptor

Introduction

Schizophrenia is a major mental disease characterized by various disturbances of perception, emotion and cognition. In the absence of any biological markers, the diagnosis is made on the basis of cross-sectional symptoms and the longitudinal course of the disease. Extensive research has been conducted to disclose the neurobiological mechanisms of schizophrenic core symptoms such as positive and negative symptoms as well as cognitive deficits. Based on a broad range of empirical findings, major pathophysiological concepts highlight, among others, aberrant salience network activity (insula and anterior cingulate cortex, ACC), prefrontal hypoactivation, sensory processing deficits as well as an impaired connectivity between temporal and prefrontal cortices. Aberrant salience network activity has been considered to underlie positive symptoms such as delusions and hallucinations due to an inappropriate assignment of salience to stimuli that would normally be considered irrelevant (Menon, 2011; Palaniyappan *et al.*, 2011, 2012).

Prefrontal cortex dysfunction is widely supposed to account for negative symptoms (Wolkin *et al.*, 1992) and cognitive deficits (Barch *et al.*, 2012) in schizophrenia, given the similarities to clinical features of patients with frontal lobe lesions. This 'hypofrontality hypothesis' is further supported by a variety of neuroimaging studies that revealed a close link between frontal hypoactivation and negative symptoms (Wolkin *et al.*, 1992; Potkin *et al.*, 2002).

A further well-documented finding in schizophrenia is early sensory processing deficits (Javitt, 2009*a*, *b*) that localize to primary and secondary sensory cortices. These deficits, present across different sensory domains, are considered to further contribute to higher order cognitive dysfunction.

Extending these concepts of localized brain dysfunctions, the dysconnection hypothesis of schizophrenia (Friston and Frith, 1995; Stephan *et al.*, 2006) emphasizes the abnormal interaction between different brain areas as the central pathogenic factor. Within this framework, disrupted functional connectivity between prefrontal and temporal cortices is considered to be of special pathophysiological significance, e.g. auditory hallucinations have been assigned to a reduced functional connectivity between the auditory cortex and the ACC (Friston and Frith, 1995).

All of the aforementioned mechanisms may underlie one of the best-replicated neurophysiological deficits in schizophrenia: the reduction of the mismatch negativity (MMN). In electroencephalography (EEG), the MMN is an event-related potential component elicited by deviants within a sequence of repetitive auditory stimuli (Näätänen, 1995). It is considered to originate in the auditory cortex. Additional contributions from the prefrontal cortex (Baldeweg *et al.*, 2002; Schall *et al.*, 2003) and the salience network (Waberski *et al.*, 2001; Schall *et al.*, 2003; Takahashi *et al.*, 2012) may initiate a subsequent involuntary switch of attention and resource allocation.

Functional MRI precisely localizes cerebral generators of the mismatch response (Mathiak *et al.*, 2002*a*; Schall *et al.*, 2003). This technique may be superior in delineating frontal mismatch deficits in schizophrenia, which topographic EEG studies found to be most prominent and specific to *N*-methyl D-aspartate receptor (NMDAR) effects (Baldeweg *et al.*, 2002; Schmidt *et al.*, 2012; Takahashi *et al.*, 2012). To our knowledge, only two studies investigated the haemodynamic analogue of auditory mismatch responses in schizophrenia; both studies were based on a relatively small number of participants and did not detect frontal activation (Wible *et al.*, 2001; Kircher *et al.*, 2004).

Resource allocation to the auditory modality, which is considered to be initiated in the prefrontal cortex, may further induce activity changes in other sensory networks (Schock *et al.*, 2013). Given the role of NMDARs for synaptic plasticity during perceptual learning, the schizophrenic mismatch impairments may also reflect a disturbed interaction (i.e. dysconnectivity) of the sensory systems with the prefrontal cortex and the salience network (Stephan *et al.*, 2006). Such distributed deficits in mismatch processing may be potent biomarkers for schizophrenia (Stephan *et al.*, 2006; Belger *et al.*, 2012), in particular,

as MMN does not depend upon directed attention or task motivation. Nevertheless, their potential for diagnostic classification has not been systematically studied yet. Previous research based on resting state functional MRI in schizophrenia suggests that functional connectivity measures can inform classifiers on disease status (Tang *et al.*, 2012). Such multivariate methods should be used to investigate the dynamic interplay of networks during mismatch processing (Stephan *et al.*, 2006) because they gather information from distributed dysfunctions and dysconnectivity. Classifiers may integrate information of independent deficits such as sensory deficits (Siegel *et al.*, 1984; Javitt, 2009*a*, *b*), aberrant salience processing (White *et al.*, 2010), and impaired connectivity (Friston and Frith, 1995; Stephan *et al.*, 2006).

The present study aimed at characterizing neural networks at high spatial resolution, which are dysfunctional during mismatch processing in schizophrenia. Therefore, by using a modified optimized mismatch design (Näätänen *et al.*, 2004; Thönnessen *et al.*, 2008), whole-brain functional MRI responses to auditory mismatch stimuli and functional connectivity were compared between patients with schizophrenia and matched control subjects. Further, classifiers assessed feature vectors with increasing dimensionality from the task-related brain activity and functional connectivity measures. This informational approach enabled to assess processing impairments at the individual patient level and disentangle the pathophysiological contributions of different neural dysfunctions to impaired mismatch processing in schizophrenia.

Materials and methods

Participants

We investigated 24 schizophrenia patients (10 female) with a mean age of 36.1 ± 9.2 years and a matched control group. The patients were recruited through the Department of Psychiatry of the University Hospital Aachen and an academically associated psychiatric clinic (Katharina Kasper Via Nobis GmbH, Hospital for Psychiatry and Psychotherapy, Gangelt, Germany). The International Classification of Diseases (ICD-10) diagnoses were ascertained by two experienced psychiatrists. Using the German version of the Structured Clinical Interview (SCID), the diagnoses were also confirmed according to Diagnostic and Statistical Manual of Mental Disorders Fourth Edition (DSM-IV) criteria in all but one patient. The latter patient was diagnosed with schizophreniform disorder, as the DSM-IV time criterion of 6 months for schizophrenia was not fulfilled. Patients with other acute psychiatric or any neurological co-morbidity were excluded. Clinical features and medication are described in Table 1.

The control group comprised 24 healthy subjects, matched for age (36.4 ± 9.3 years), gender (10 female), and parental education. All but one participant were right-handed as rated by the Edinburgh Handedness Inventory. The experimental protocol was approved by the local Ethics Committee of the RWTH Aachen University Hospital. Written informed consent was obtained from all participants, following a complete description of the study.

Stimuli

In the modified optimized mismatch design, auditory stimulation comprises one standard and five types of deviant tones (Näätänen *et al.*, 2004; Thönnessen *et al.*, 2008). All stimuli were spectrally rich tones synthesized by three sinusoidal partials with the second and third partials being softer by 3 and 6 dB, respectively (Tervaniemi *et al.*, 2000). The standard tones comprised partials at 500, 1000 and 1500 Hz, lasted 100 ms, and were presented binaurally via headphones at 90 dB sound pressure level. The five deviant types (10% each) differed from the standard stimulus with regard to exactly one of the following five features, leaving the others in 90% of the events in their standard configuration: (i) frequency – half of the frequency deviants were 33% higher (667, 1333 and 2000 Hz) and another half 33% lower (333, 667, and 1000 Hz) than the standard stimulus; (ii) duration – deviants were either half as long (50 ms) or twice as long (200 ms) as the standard stimulus; (iii) amplitude – deviants were 10 dB louder or 10 dB softer than the standard stimulus; (iv) gap – deviants were created by including a pause of 25 or 50 ms in the middle of the standard stimulus; and (v) location – deviants featured an interaural time difference of 1 ms and a matching interaural amplitude difference of 3 dB in favour of the left or the right channel. The perceived azimuth of the sound source resulted as ∼90° to the left or the right side, whereas the standard binaural stimulus was perceived in the centre. All auditory stimuli were generated using Matlab 2011b software (Mathworks).

Experimental design

The functional MRI paradigm had a total duration of 8 min. In a block design, eight standard blocks with 30-s duration each comprised only the standard stimuli and eight mismatch blocks (also 30-s duration) comprised standard and deviant stimuli. Each of the five types of deviants was presented with a probability of 10%, yielding a probability of 90% for each feature to be presented in its standard value. The auditory stimuli were presented at a constant stimulus onset asynchrony of 500 ms resulting in 60 stimuli per block.

The structure of the mismatch blocks was adopted from the optimized mismatch paradigm (Näätänen *et al.*, 2004). This paradigm was chosen because in the previous comparative EEG- MEG (magnetoencephalography) study, it was more sensitive to the deficit in schizophrenia in comparison to a standard oddball paradigm with deviants in 20% of the stimuli only (Thönnessen *et al.*, 2008; Zvyagintsev *et al.*, 2008). The two variants of each deviant type were presented with equal probability. Within the mismatch blocks, the deviants were presented as every second stimulus with the restriction that two deviants of the same category never followed each other (Fig. 1). The participants were instructed to ignore the auditory stimuli and to watch a movie played without sound (Koyaanisqatsi, Godfrey Reggio, IRE Productions, NM, 1982).

Data acquisition

MRI was conducted using a 3 T Tim Trio Scanner (Siemens) with a 12-channel head coil. Anatomical reference imaging applied a T_1-weighted 3D sequence (echo time = 2.98 ms; repetition time = 2 300 ms; inversion time = 900 ms; flip angle = 9°; field of

Table 1 Sociodemographic characteristics of schizophrenia patients and healthy control subjects

Characteristic	Controls ($n = 24$)		Patients ($n = 24$)		Comparison	
	Mean	SD	Mean	SD	$t(df = 46)$	P
Age (years)	36.4	9.3	36.1	9.2	0.13	0.90
Education (years)[a]	16.3	3.0	15.0	2.5	1.57	0.12
Parental education (years)	12.9	2.5	12.5	2.9	0.61	0.54
Fagerström Test for Nicotine Dependence score[b]	0.4	1.4	2.1	2.9	**−2.56**	**0.01**
Digit Span Test score	17.5	3.6	15.8	3.9	1.51	0.14
Mehrfachwahl-Wortschatz-Intelligenz-Test score[c]	32.0	3.1	29.9	4.3	1.96	0.06
Regensburger Wortflüssigkeits-Test-K score[d]	13.6	3.4	12.1	4.7	1.30	0.20
Regensburger Wortflüssigkeits-Test-G-R score[d]	14.0	3.5	11.0	4.5	**2.53**	**0.02**
Trail-Making Task B (s)	41.9	14.2	52.7	19.4	**−2.21**	**0.03**
Duration of illness (years)			8.3	8.2		
Positive and Negative Symptom Scale scores						
Positive symptoms			10.4	3.0		
Negative symptoms			11.5	4.1		
General psychopathology			21.4	4.0		
Total			43.3	9.4		
Medication (percentage of defined daily dose):						
Antipsychotics, $n = 23$			156.9	77.3		
Antidepressants, $n = 8$			127.1	58.9		
	n	%	n	%	χ^2 $(df = 1)$	P
Gender					0.0	1.00
Male	14	58.3	14	58.3		
Female	10	41.7	10	41.7		
Handedness						1.00[e]
Right	24	100.0	23	95.8		
Left	0	0.00	1	4.2		

[a]Including formal 3-year job apprenticeship with compulsory 1 day/week school attendance and university education.
[b]The Fagerström Test for Nicotine Dependence (FTND) is a screening instrument for nicotine dependence.
[c]The Mehrfachwahl-Wortschatz-Intelligenztest (MWT-B) is a German multiple choice vocabulary intelligence test estimating subjects' verbal crystallized intelligence.
[d]The Regensburger Wortflüssigkeits-Test (RWT) is a German verbal fluency test.
[e]Fisher's exact test, two-tailed P-value.

view = 256 × 256 mm^2; voxel size = 1 × 1 × 1 mm^3; 176 sagittal partitions). Echo-planar imaging obtained T_2*-weighted images of the whole brain (echo time = 36 ms; repetition time = 1800 ms; flip angle = 72°; voxel size = 3 × 3 × 4 mm^3; gap = 0.5 mm; field of view = 192 × 192 mm^2; matrix size = 64 × 64; interleaved acquisition of 26 transverse slices).

Preprocessing

Functional MRI data analysis was performed using BrainVoyager QX 2.6 (Brain Innovation) and Matlab 2011b (Mathworks). The first five images of each run were discarded. The preprocessing included: slice-time correction, mean intensity adjustment, motion correction, spatial smoothing (6 mm full-width at half-maximum Gaussian kernel) and temporal high-pass filtering (0.006 Hz). Adapting the data to the functional connectivity analysis, the functional MRI time courses were further corrected by regressing out the average signals obtained from the white matter, CSF and a region outside the brain. Head motion parameters and a discrete cosine function set were also included in the regression model. After preprocessing, functional data were co-registered to the individual high-resolution anatomical images. Both the anatomical and functional images were transformed into Talairach space.

General linear model analysis

Functional MRI data were subjected to a general linear model (GLM) analysis. The mismatch condition served as the predictor of interest and was modelled with a boxcar function convolved with the canonical haemodynamic response function; the standard condition served as a baseline. The beta estimates from the individual GLMs entered a second level random effects analysis. Contrast maps were created by applying paired t-tests comparing the mismatch versus standard (baseline) condition for each group separately as well as a two sample t-test for the between-groups comparison. The threshold was set to $P < 0.05$ for a cluster size threshold, which was estimated by a Monte-Carlo simulation based on 10 000 iterations (Forman *et al.*, 1995).

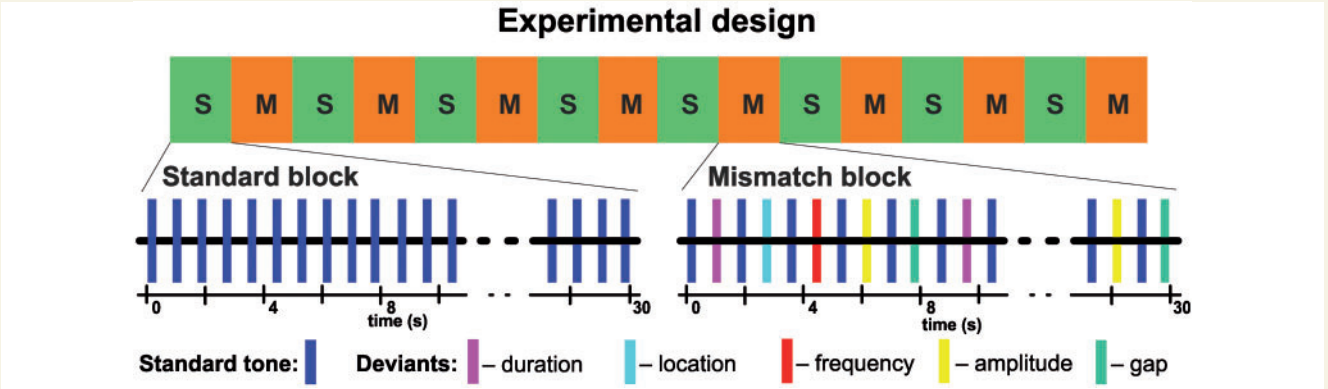

Figure 1 Schematic illustration of the optimized mismatch paradigm applied in this study. In a block design (8 min), presentation of standard events (tone with complex partials, 100 ms duration, stimulus onset asynchrony = 500 ms) served as baseline (S; 30 s duration each block). During mismatch blocks (M; 30 s), every second event varied in one randomly chosen feature, i.e. either in duration, location, frequency, amplitude or an introduced gap.

Psychophysiological interaction analysis

Psychophysiological interaction analysis addressed condition-dependent functional connectivity between the auditory cortex and the ACC (Friston *et al.*, 1997; SPM8 software: www.fil.ion.ucl.ac.uk). Regions of interest were defined according to the automated anatomical labelling atlas (Tzourio-Mazoyer *et al.*, 2002). Average region of interest signals were extracted from the high-pass filtered volume time series and normalized. The psychophysiological interaction analysis calculated individual functional connectivity between the left and right Heschl's gyrus and the ACC as well as its modulation by the experimental condition (mismatch versus standard condition). Repeated-measures analysis of variance (ANOVA) investigated condition and side (left versus right Heschl's gyrus) as intrasubject as well as group as intersubject factors. Fisher's least significant difference test was applied as *post hoc* test.

Classifiers

As information-based procedure to determine differences in brain activity between patients and controls, we applied a classifier algorithm. Therefore, a modified support vector machine algorithm (Tang *et al.*, 2012; Zeng *et al.*, 2012) was applied to two data sets: (i) condition-dependent brain activity as reflected by the beta estimates of the GLM analysis (see also Dinkel *et al.*, 2013); and (ii) functional connectivity measured by a correlation analysis across the whole brain. For both data sets, the cerebrum was divided into the same 90 regions of interest (45 in each hemisphere) according to the automated anatomical labelling atlas (Tzourio-Mazoyer *et al.*, 2002). In the GLM-based approach, averaged beta values from the mismatch condition were extracted from each region of interest, resulting in 90 features per subject. In the functional connectivity-based approach, time series were extracted from each region of interest and Fisher's *z*-transformed Pearson correlation coefficients were calculated for each pair of regions. Thereby, we obtained a 90×90 correlation matrix. Removing 90 diagonal elements, the upper triangle of the matrix was extracted, resulting in 4005 functional connectivity features per participant.

A filtering and information-based feature selection procedure was applied and a variable number of target features entered the classifier (Kachel *et al.*, 2010). First, a filter selected features exhibiting the most variance. Thereto, the features were ranked based on their range, i.e. the difference between maximum and minimum, and at least 90 or the 2.5-fold of the number of target features were selected. This procedure ensured stability of the information-based feature selection and made the GLM and functional connectivity condition more comparable. Second, an information-based feature selection ranked the features according to absolute value of the Kendall-Tau rank correlation coefficients (Kendall and Jean, 1990) and a variable number of target features was selected, which exhibited highest relation to the group indicator. Third, the classifier applied support vector machines with a linear kernel (Bishop, 2006). Therefore, the support vector machine yielded a maximal-margin hyperplane in the feature space, which separated the groups in a training data set. Classification was tested in the left-out sample. The limited number of subjects lent to the leave-one-out cross-validation method to investigate the generalizability of the classification results. This cross-validation encompassed the feature filtering and selection as well as the classifier. Accuracy (percentage of participants detected correctly), sensitivity (percentage of schizophrenia patients detected correctly), and specificity (percentage of controls detected correctly) quantified classification performance.

Results

General linear model analysis

Control subjects demonstrated activation to mismatch blocks in bilateral auditory cortices comprising Heschl's and superior temporal gyri ($t_{peak\ voxel} = 15.77$, right superior temporal gyrus). Further, activity emerged at the prefrontal cortex (right inferior frontal gyrus, bilateral middle

and superior frontal gyrus), the salience network (bilateral insula and ACC / medial frontal gyrus) and posterior portions of the default mode network (bilateral posterior cingulate cortex, precuneus and angular gyrus). Furthermore, deactivation was observed in the visual system—comprising the occipital pole as well as portions of the ventral (bilateral fusiform and inferior temporal gyrus) and the dorsal stream (bilateral inferior and superior parietal lobule)—and in the dorsal attention network (bilateral intraparietal sulcus and frontal eye fields) as well as the bilateral pre- and postcentral gyrus. For details see Fig. 2A and Table 2.

The schizophrenia group yielded activation in bilateral auditory cortices as well but statistics appeared lower at the right auditory cortex (Table 2). Further, left pre- and postcentral gyri were activated except for one cluster comprising the left inferior and middle frontal gyrus, prefrontal brain areas, and insula failed yielding significant clusters. Moreover, the deactivation of the visual system was less extended (k = 17 539 versus 83 305 voxels in controls) and no significant deactivation in the dorsal attention network emerged (Fig. 2B and Table 2).

The group differences were confirmed in the direct comparison: patients with schizophrenia exhibited less activation in the right auditory cortex including Heschl's and superior temporal gyrus compared to healthy controls [t_{peak} = 3.98 at (62, −23, 3)]. Furthermore, lower activity emerged in the prefrontal cortex encompassing the right inferior frontal gyrus, bilateral middle and superior frontal gyrus as well as the salience network (bilateral ACC, medial frontal gyrus and right insula). Interestingly, the observed deactivation patterns were also less prominent in the patients, i.e. in visual areas comprising the occipital pole, bilateral ventral and left dorsal stream as well as in the left dorsal attention network (intraparietal sulcus). Finally, the left pre- and postcentral gyrus was significantly higher activated in the patient group (Fig. 2C and Table 2).

Psychophysiological interaction analysis

The ACC is considered a control structure for auditory processing (Friston and Frith, 1995) and exhibited the strongest group difference in the GLM analysis. The psychophysiological interaction analysis, therefore, investigated its functional connectivity with both auditory cortices (left and right Heschl's gyrus). A significant condition-group interaction emerged [$F(1,46) = 7.45$, $P = 0.007$]. The other effects and interactions failed significance in the ANOVA [all $F(1,46) < 1.00$, $P > 0.4$]. *Post hoc* Fisher's least significant difference test revealed a significant difference in functional connectivity between the mismatch and standard conditions only in healthy controls ($P = 0.01$) and between the groups in the mismatch condition ($P = 0.04$).

Classifiers

Cross-validation of the classifier using GLM data yielded a maximal accuracy of 83% (sensitivity 83%, and specificity 83%) with four features. No further improvement emerged

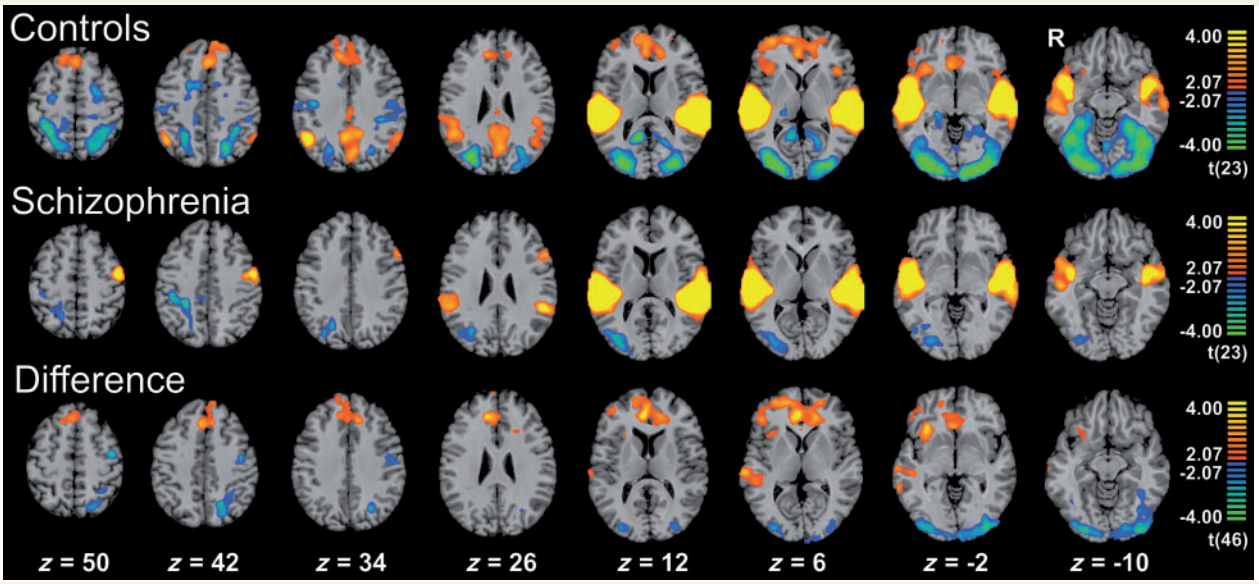

Figure 2 Haemodynamic response to mismatch blocks. Activation clusters of healthy controls (n = 24; first row), schizophrenia patients (n = 24; second row) and healthy controls > schizophrenia patients (third row) for the contrast mismatch > standard (baseline) condition. Both groups exhibited prominent auditory activations, which differed at the right auditory cortex. Prefrontal and salience network responses were only observed in the control group yielding a significant group difference. The deactivation in the visual system was significantly stronger in the controls. For each contrast, the threshold was set to $P < 0.05$ and a corrected cluster size threshold based on a Monte-Carlo simulation was applied. z-coordinates refer to the Talairach system.

Table 2 Local maxima of significant activation clusters

Anatomic area	Healthy controls (n = 24)				Patients (n = 24)				Healthy controls > Patients			
	Talairach coordinates			t-score	Talairach coordinates			t score	Talairach coordinates			t score
	x	y	z	(df = 23)	x	y	z	(df = 23)	x	y	z	(df = 46)
Auditory system												
L. Heschl's gyrus	−43	−23	6	11.29	−37	−31	12	11.49				
R. Heschl's gyrus	53	−12	3	13.22	50	−19	9	10.67	53	−11	6	2.49
L. sup. temporal gyrus	−4	−23	6	11.93	−55	−26	9	13.83				
R. sup. temporal gyrus	59	−26	9	15.77	50	−26	12	11.24	62	−23	3	3.98
Prefrontal cortex												
L. inf. frontal gyrus					−55	16	30	4.33				
R. inf. frontal gyrus	50	11	−2	4.18					44	34	6	3.44
L. mid. frontal gyrus	−24	1	60	−4.22	−51	13	34	3.36	−24	50	6	2.48
R. mid. frontal gyrus	32	52	6	4.81					38	10	45	3.94
L. sup. frontal gyrus	−19	1	57	−5.69					−12	31	36	4.13
R. sup. frontal gyrus	32	53	7	4.33					17	52	6	3.66
Salience network												
L. anterior cingulate cortex	−13	40	15	4.36					0	37	3	4.19
R. anterior cingulate cortex	5	37	6	4.40					5	37	6	4.82
L. medial frontal gyrus	−10	31	39	4.71					−10	31	36	4.52
R. medial frontal gyrus	11	37	36	4.50					3	28	45	4.20
L. insula	−38	19	6	3.53								
R. insula	32	25	0	3.79					34	16	0	4.15
Visual system (occipital pole)												
L. inferior occipital gyrus	−34	−86	−6	−5.91					−34	−88	−6	−4.47
R. inferior occipital gyrus	35	−83	−9	−6.31	31	−82	−6	−3.39	38	−83	−6	−4.02
L. middle occipital gyrus	−34	−86	−2	−5.74	−31	−86	21	−3.95	−40	−89	−5	−4.47
R. middle occipital gyrus	35	−86	7	−5.70	29	−66	27	−3.89	30	−86	0	−3.46
L. superior occipital gyrus	−13	−92	1	−5.26	−22	−68	22	−3.21	−23	−66	33	−3.43
R. superior occipital gyrus	25	−74	21	−5.22	29	−74	15	−3.79	20	−95	4	−2.77
L. cuneus					−15	−86	36	−2.62				
R. cuneus	20	−85	9	−4.18	18	−65	33	−3.43	15	−98	4	−2.10
L. calcarine	−10	−92	−3	−5.40	−13	−86	6	−2.91	−7	−98	−3	−3.54
R. calcarine	24	−90	−1	−5.13	21	−80	4	−3.09	10	−97	−6	−3.30
L. lingual gyrus	−14	−89	−3	−4.91					−34	−89	−15	−3.90
R. lingual gyrus	25	−89	−6	−5.91	24	−78	0	−3.24	23	−86	−12	−4.17
Visual system (ventral stream)												
L. inferior temporal gyrus	−46	−62	−6	−4.94					−42	−49	−12	−2.96
R. inferior temporal gyrus	41	−54	−9	−4.87	47	−68	−6	−3.40	39	−61	−12	−2.96
L. fusiform gyrus	−37	−50	−12	−5.47					−37	−50	−12	−3.85
R. fusiform gyrus	29	−86	−6	−6.09	24	−41	−12	−4.08	24	−86	−12	−4.05
Visual system (dorsal stream)												
L. inferior parietal lobule	−31	−56	45	−4.81					−34	−47	48	−2.80
R. inferior parietal lobule	44	−53	37	4.92	27	−51	54	−3.06				
L. superior parietal lobule	−22	−65	45	−4.86					−19	−59	42	−3.90
R. superior parietal lobule	35	−44	51	−4.88								
Dorsal attention network												
L. intraparietal sulcus	−21	−65	48	−4.17					−22	−68	48	−3.16
R. intraparietal sulcus	26	−60	48	−4.60								
L. frontal eye field	−25	−8	50	−3.74								
R. frontal eye field	26	−14	48	−3.70								
Default mode network (posterior nodes)												
L. precuneus	7	−65	30	4.37								
R. precuneus	5	−53	33	4.62								
L. posterior cingulate	−4	−53	21	3.96								
R. posterior cingulate	5	−50	30	4.13								
L. angular gyrus	−49	−68	31	4.40								
R. angular gyrus	44	−53	36	5.19								

(continued)

Table 2 Continued

Anatomic area	Healthy controls (n = 24)				Patients (n = 24)				Healthy controls > Patients			
	Talairach coordinates			t-score	Talairach coordinates			t score	Talairach coordinates			t score
	x	y	z	(df = 23)	x	y	z	(df = 23)	x	y	z	(df = 46)
Sensorimotor cortex												
L. precentral gyrus	−28	−26	60	−3.34	−49	−5	45	5.55	−40	−11	54	−5.65
R. precentral gyrus	39	−14	36	−4.63								
L. postcentral gyrus	−20	−44	66	−4.42	−46	−14	48	5.71	−45	−11	36	−3.72
R. postcentral gyrus	26	−41	63	−5.03								

L. = left, R. = right. Anatomical labels were obtained using the automated anatomical labeling atlas. Labels for areas belonging to the same gyrus were concatenated under the label of the respective gyrus. Since the dorsal attention network (bilateral intraparietal sulcus and frontal eye field) is not included in the automated anatomical labeling atlas, the respective regions were defined as 8 mm (diameter) spheres centered on previously published foci (31) : (x,y,z) = (−23, −66, 51) for the left intraparietal sulcus; (24, −63, 49) for the right intraparietal sulcus, (−23, −11, 49) for the left frontal eye field and (28, −12, 49) for the right frontal eye field.

with increasing numbers of features (Fig. 3). As compared to the GLM result, the functional connectivity classifier performed similarly or worse for up to ∼10 features. However, an improvement was observed after inclusion of >10 features and ⩾24 features yielded a maximal accuracy of 90% (sensitivity 88% and specificity 92%).

In a further analysis, we studied features that were consistently selected across the cross-validation procedure. As concerns the GLM data, the ACC was the most discriminative feature followed by the middle frontal gyrus and inferior occipital gyrus (Table 3). Among the 20 most discriminating functional connectivity features, 17 features reflected correlations between brain signals exhibiting task-related responses in the GLM analysis (Table 4); six of these features reflected connectivity between auditory and prefrontal cortex or salience network (Features 4, 6, 8, 10, 16 and 20 in Table 4). The remaining features involved prefrontal and visual areas, the paracentral lobule as well as frontostriatal connections.

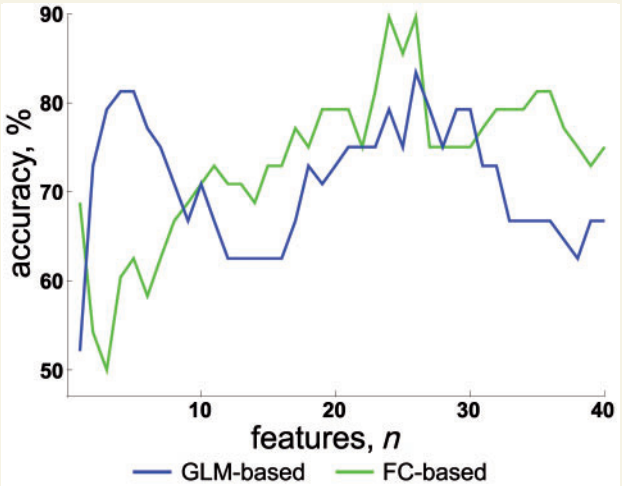

Figure 3 Information increase for many functional connectivity features. Classification accuracy depending on the number of selected features from GLM effect estimates (blue line) and functional connectivity measures (green line). Already based on few features from the region of interest activation (GLM analysis), accuracy was ∼80%; this rate is similar to other MMN studies (e.g. Thönnessen *et al.*, 2008). For connectivity features, higher numbers of features led to still higher classification accuracy (up to 90%), suggesting distributed contribution of network dysfunction to schizophrenia.

Discussion

We investigated the haemodynamic analogue of auditory mismatch processing in patients with schizophrenia and healthy participants. In addition to the well-documented hyposensitivity of auditory areas to the mismatch detection, schizophrenia was associated with a reduced activity of prefrontal (inferior, middle and superior frontal gyri) and salience networks (insula and ACC extending into medial frontal gyri). Further, the associated deactivation of visual processing areas was reduced in the patients. These impaired responses to the deviant auditory stimuli across a distributed network yielded ∼80% classification accuracy. However, additional information for the group discrimination emerged from functional connectivity measures. First, functional coupling between the auditory cortices and ACC was diminished in the patients. Second, inclusion of functional connectivity measures across the distributed networks yielded higher classification accuracy. In summary, pathophysiology of unattended deviant processing in schizophrenia is characterized by distributed dysconnectivity in addition to deficient processing at auditory and prefrontal cortices as well as the salience network.

Auditory system

Impaired mismatch processing is a well-documented neurophysiological deficit in schizophrenia (reviewed in Javitt, 2009*a*, *b*). The optimum mismatch design is a variant with a high number of deviant events, and it can also detect processing deficits in schizophrenia using EEG and MEG (Thönnessen *et al.*, 2008). This study documented for the first time haemodynamic brain responses to an adapted optimum design and the associated processing deficit in

Table 3 Most discriminating features from GLM analysis

Number	Region	Kendall Tau τ
1	R. anterior cingulate cortex	0.57
2	R. middle frontal gyrus, orbital portion	0.56
3	L. inferior occipital gyrus	−0.52
4	R. inferior occipital gyrus	−0.52
5	L. superior parietal lobule	−0.48
6	R. medial frontal gyrus	0.44
7	L. middle occipital gyrus	−0.43
8	R. superior temporal gyrus	0.42
9	L. anterior cingulate cortex	0.41
10	R. middle frontal gyrus	0.40
11	R. insula	0.39
12	L. fusiform gyrus	−0.39
13	L. precentral gyrus	−0.39
14	L. Thalamus	0.38
15	R. fusiform gyrus	−0.35
16	L. medial frontal gyrus	0.34
17	L. calcarine	−0.34
18	L. superior frontal gyrus, orbital portion	0.33
19	R. middle occipital gyrus	−0.33
20	R. calcarine	−0.33

L. = left, R. = right. A positive correlation coefficient τ indicates that the feature was larger in the control group compared to the patient group, whereas a negative correlation coefficient indicates that it was larger in the patient group.

schizophrenia. At the corrected threshold, patients exhibited reduced responses in the right but not the left auditory cortex. Such a right lateralized deficit is consistent with the previous comparative functional MRI-MEG study, which documented a reduced right-hemispheric lateralization of mismatch responses in patients with corresponding haemodynamic and electrophysiological measures (Kircher *et al.*, 2004). This lateralization pattern may reflect higher right-hemispheric proficiency for tone processing (e.g. Mathiak *et al.*, 2002*b*). However, lateralization may depend on stimulus and deviant type, e.g. pure tones with frequency deviants elicited left dominant MMN responses in healthy control subjects as well as left dominant deficits in patients with schizophrenia (Park *et al.*, 2002). The haemodynamic analogue of mismatch responses thus is in agreement with a model of sensory processing deficits at the level of the auditory cortex in schizophrenia.

Frontal and salience networks

The control group further exhibited widespread activation of prefrontal brain areas including inferior, middle, and superior frontal gyri. With respect to mismatch processing, prefrontal activation has been considered to reflect mechanisms for attention shifts triggered by the auditory change detection (Näätänen, 1995; Schall *et al.*, 2003)—potentially as a result of further processing according to a prediction error hypothesis (Winkler *et al.*, 1996). Compared to controls, patients exhibited significantly lower activation across the entire prefrontal cortex in agreement with previous EEG studies (Baldeweg *et al.*, 2002; Takahashi *et al.*, 2012). Notably, the two previous functional MRI studies on mismatch responses in schizophrenia failed to reproduce this finding (Wible *et al.*, 2001; Kircher *et al.*, 2004). Conceivably, the higher number of participants and the optimized mismatch design yielded the confirmation of reduced frontal activation by functional MRI. The optimum design may be associated with high mismatch amplitudes (Thönnessen *et al.*, 2008) and MMN deficits in schizophrenia were particularly marked for deviants with high MMN amplitudes (Javitt *et al.*, 1998; Shelley *et al.*, 1999; Sato *et al.*, 2003). Todd *et al.* (2012) argued that such a lowered dynamic range to respond to deviant stimuli may interfere with associating salience to relevant cues and thereby affecting processing at higher cognitive levels.

The group differences were most pronounced in the medial frontal gyrus and the ACC similar to a recent EEG study with 410 patients with schizophrenia (Takahashi *et al.*, 2012). In addition, our patients exhibited a reduced functional connectivity between auditory cortex and ACC. Indeed, the most discriminating features for the functional connectivity-based classifier comprised connections between bilateral auditory and frontal regions such as the superior frontal gyrus, medial frontal gyrus, and ACC (Table 4). Therefore, the present results support the view that the prominent mismatch processing deficit in the frontal areas may be in part explained by dysconnectivity between temporal and frontal brain structures (Friston and Frith, 1995; Stephan *et al.*, 2006). Reciprocal anatomical connections between these regions may serve stimulus-driven orienting of attention (Barbas *et al.*, 1999). Dysconnectivity in schizophrenia may manifest as the symptomatic attention deficit.

Controls activated the anterior insula more than patients during mismatch processing. The anterior insula in conjunction with the ACC and the medial frontal cortex constitute the salience network (Seeley *et al.*, 2007). In a stimulus-rich environment, the salience network subserves ‘to identify the most homeostatically relevant among these myriad inputs’ (Seeley *et al.*, 2007), and thus allows allocating attentional resources for orienting towards relevant stimuli. Recently, the salience network has been considered as a neural substrate of the aberrant salience model which represents one of the most influential contemporary models of positive symptoms in schizophrenia (Kapur, 2003). This model proposes that positive symptoms arise from inappropriate assignment of salience to stimuli which would normally be considered irrelevant. At the neural level, excessive dopaminergic signalling within the mesolimbic circuit and, recently, a dysfunction of the salience network (Menon, 2011; Palaniyappan *et al.*, 2011, 2012) have been considered to underlie aberrant salience attribution to external events and internal representations, thus leading to delusions and hallucinations, respectively. Indeed, a variety of studies have revealed a close relationship between aberrant salience network activity and positive symptoms in

Table 4 Most discriminating features from the functional connectivity analysis

Number	Region 1	Region 2	Kendall Tau τ
1	L. fusiform gyrus	R. fusiform gyrus	0.59
2	L. lingual gyrus	R. paracentral lobule	−0.55
3	R. caudate nucleus	L. supplementary motor area	0.54
4	R. superior frontal gyrus	R. Heschl's gyrus	0.53
5	R. amygdala	L. paracentral lobule	−0.53
6	R. anterior cingulate cortex	L. Heschl's gyrus	0.52
7	R. inferior frontal gyrus, orbital portion	L. middle occipital gyrus	0.52
8	L. anterior cingulate cortex	L. Heschl's gyrus	0.52
9	R. lingual gyrus	R. paracentral lobule	−0.51
10	L. medial frontal gyrus	L. Heschl's gyrus	0.50
11	R. inferior frontal gyrus, pars triangularis	R. middle occipital gyrus	0.49
12	R. caudate nucleus	R. supplementary motor area	0.49
13	L. fusiform gyrus	R. inferior occipital gyrus	0.49
14	L. posterior cingulate cortex	L. paracentral lobule	0.49
15	L. cuneus	L. temporal pole, superior portion	0.49
16	R. anterior cingulate cortex	L. superior temporal gyrus	0.48
17	L. caudate nucleus	L. superior frontal gyrus	0.48
18	R. lingual gyrus	R. postcentral gyrus	−0.48
19	R. inferior frontal gyrus, orbital portion	R. middle frontal gyrus, orbital portion	−0.48
20	R. medial frontal gyrus	R. Heschl's gyrus	0.47

L. = left, R. = right. A positive correlation coefficient τ indicates that the feature (functional connectivity measure) was larger in the control group compared to the patient group, whereas a negative correlation coefficient indicates that it was larger in the patient group.

schizophrenia (Liddle *et al.*, 1992; Jardri *et al.*, 2011; Palaniyappan *et al.*, 2011). Within the framework of predictive coding models, the chaotic neural activity underlying aberrant salience attribution has been considered to manifest as aberrant encoding of prediction errors (Fletcher and Frith, 2009). Predictive coding models assume hierarchical neural systems where each level receives bottom-up information about sensory input from the level below and top-down predictions about that input from the level above. A prediction error refers to a mismatch between the incoming sensory information (bottom-up input) and prior expectation (top-down prediction). Notably, the salience network has been repeatedly shown to be involved in prediction error coding (Kennerley *et al.*, 2006; Clark *et al.*, 2008; Murray *et al.*, 2008; Preuschoff *et al.*, 2008). Lieder *et al.* (2013) conducted a formal cross-comparison of all major MMN theories. Using a Bayesian framework, models based on the free energy principle, such as the prediction error model (Garrido *et al.*, 2009), provided a more plausible explanation of trial-by-trial changes in the MMN amplitude in a roving paradigm. According to that model, MMN is a prediction error signal, resulting from a mismatch between the auditory input (deviant) and a predictive memory trace.

Different sources of evidence suggest a link between dopaminergic signalling and the salience network (for a review, see Palaniyappan *et al.*, 2012), e.g. both the insula and ACC exhibit a relatively high density of extrastriatal dopamine transporters (Wang *et al.*, 1995). Furthermore, a PET study revealed a positive correlation between the binding potential of the dopamine D2/D3-receptor ligand ^{18}F-fallypride and grey matter density in both regions (Woodward *et al.*, 2009). However, MMN was not influenced by dopaminergic-modulations as measured by EEG and MEG (Kähkönen *et al.*, 2001, 2002; Pekkonen *et al.*, 2002; Leung *et al.*, 2007, 2010). Conceivably, the EEG/MEG-signal of the MMN is dominated by generators from the auditory cortex. This, however, has not been studied with respect to the haemodynamic analogue of the MMN, which may reflect later and dopamine-mediated processes. The involvement of the salience network as observed in our study may reflect higher order processes which are secondary to deviant detection, e.g. the integration of the prediction error signalling in adequate behavioural responses or attention shifts.

Other sensory systems

Control subjects exhibited deactivation of visual and sensorimotor areas. Suppression of the visual cortex during auditory mismatch processing has been observed previously (Schock *et al.*, 2012). Such a finding can be interpreted in line with the classical suggestion of automatic attention allocation in mismatch processing (Näätänen, 1995; Schall *et al.*, 2003). Similarly, recent computational models suggest mismatch responses to indicate prediction errors (Lieder *et al.*, 2013), and this 'signal, after further processing, may participate in the directing of attention' (Winkler *et al.*, 1996). Such an error signal enables focal resource allocation for capacity sharing (Tombu and Jolicoeur,

2003). Indeed a shift of resources away from the visual towards the auditory domain during mismatch processing has been found in a behavioural experiment (Schock *et al.*, 2013). Along those lines in our experiment, the healthy participants deactivated the dorsal attention network (Corbetta and Shulman, 2002; Kincade *et al.*, 2005) and the default mode network became more active. Activity of the dorsal attention network is associated with selective attention towards the visual modality and is anti-correlated to the activity of the default mode network (Fox *et al.*, 2005). Considering the physiological mechanisms of these distributed networks in healthy controls, reduced modulation of the visual system and the dorsal attention network in the patients underscores the relevance of disturbed mismatch processing for distributed network functions.

Classifiers

To further disentangle the pathophysiological contributions of the distributed neuronal activity during mismatch processing to schizophrenia, a classifier analysis investigated the contribution of an increasing number of features. Already four features obtained from the GLM analysis allowed for over 80% classification accuracy. Such classification rates are in agreement with previous studies applying a variety of classifiers to functional MRI (Demirci *et al.*, 2008; Shen *et al.*, 2010) and other neurophysiological data (Thönnessen *et al.*, 2008). These numbers also underpin that brain imaging data may serve as robust endophenotypes. However, such performance is not satisfactory for diagnostic or screening tests.

Functional connectivity data yielded high diagnostic accuracy, e.g. 94.3% for major depression (Zeng *et al.*, 2012). Similarly, when allowing for 24 or more functional connectivity features, our schizophrenia group was detected with 90% accuracy. This may be a conservative estimation and a further potential remains to improve classification performance for a better preselection of features. So far, an even higher accuracy has been previously reported using eye tracking data only (Benson *et al.*, 2012). A discussion in how far such measures would provide a reproducible and generalizable test which is selective for schizophrenia is beyond the scope of the current study. Nevertheless, the implications for the observed pathophysiology are noteworthy. In the classification analysis, functional connectivity features from distinct neural networks contribute to the separation of patients with schizophrenia and control participants. This may be taken as an indicative that in the individuals different profiles of disturbed connectivity are present. Accordingly not only sensory deficits and resulting higher order processing deficits would be associated with schizophrenia but dysconnectivity may contribute to a variable degree to impaired mismatch processing.

Altered connectivity is a consistent finding in schizophrenia (Friston and Frith, 1995), which may reflect aberrant NMDAR-dependent synaptic plasticity (Stephan *et al.*, 2006). Notably, MMN deficits were found after application of the NMDAR antagonist ketamine—both locally in primate auditory cortices (Javitt *et al.*, 1996) and systemically in humans (Umbricht *et al.*, 2002). The sensory processing deficits in schizophrenia (Siegel *et al.*, 1984; Javitt, 2009*a*, *b*) may just reflect the dysconnectivity and MMN paradigms may be useful to study synaptic plasticity during perceptual learning (Stephan *et al.*, 2006). Further, NMDAR-dependent synaptic plasticity is modulated by different neurotransmitters such as acetylcholine, dopamine and serotonin (Stephan *et al.*, 2006). Consequently, different pathways may contribute to such aberrant synaptic plasticity in schizophrenia. Whereas dopaminergic manipulation does not conceivably affect the MMN amplitude (see above), a serotonergic effect was confirmed in different studies which revealed an increase of the MMN amplitude by SSRIs (selective serotonin reuptake inhibitors) (Wienberg *et al.*, 2010).

The cholinergic system plays a central role in models of perceptual learning (Friston, 2005) but had varying effects on mismatch responses: a single dose of the muscarinic receptor antagonist scopolamine yielded decreased MMN amplitudes in young healthy subjects (Pekkonen *et al.*, 2001) but not in elderly (Pekkonen *et al.*, 2005). In contrast, nicotinergic stimulation increased the MMN amplitude in a group of healthy subjects (Harkrider *et al.*, 2005), but in another study nicotinergic effects depended on baseline MMN amplitudes (Knott *et al.*, 2014). In patients with schizophrenia, exposure to nicotine did not affect the MMN amplitude (Fisher *et al.*, 2012). Thus, different mechanisms seem to influence the cholinergic modulations of MMN generators. In summary, the complementing information from various networks to the diagnostic classifier suggests synergistic deficits in bottom-up and salience processing as well as wide-spread dysconnectivity.

Limitations

In this study, all patients received psychotropic medication. Hence, medication effects cannot be excluded. Nevertheless, the mismatch deficit in schizophrenia persists irrespective of neuroleptic medication (Catts *et al.*, 1995) and antidepressants such as SSRIs even increased the MMN (Wienberg *et al.*, 2010). Therefore, it is unlikely that the findings reflect mere medication effects. However, only a systematic study on medicated, unmedicated and medication-naive patients may resolve this ambiguity. Further, the limited temporal resolution of functional MRI does not allow for separation of responses to the different deviant types as well as the different neurophysiological components such as N1 (fronto-central negativity 100 ms after sound onset), MMN, P2b (positive potential about 200 ms after onset), or P3a (before 300 ms after oddball) emerging at different latencies. Conceivably, the current experiment integrates all the effects and thus may show processing deficits to different types of deviants at different processing levels and in different neurotransmitter systems.

The spatial patterns of the detected networks span those described in Takahashi *et al.* (2012) for both the MMN and the subsequent P3a. Finally, the resampling based cross-validation suffers the risk of biased estimators and a cross-validation in an independent sample would be required to corroborate the performance measures of neuroimaging-based classifiers.

Conclusion

Schizophrenic symptoms manifest in different phenotypes. Among others, aberrant salience network activity, sensory processing deficits, prefrontal hypoactivation as well as prefrontal-temporal dysconnectivity are discussed as underlying neural mechanisms. Our findings suggest that the well-documented MMN reduction in schizophrenia may reflect a direct consequence of each of them. Functional MRI disentangled the different neural networks, which are impaired during mismatch processing in schizophrenia. Specifically, for a subset of features in most of the patients, the classifier detected some characteristics of altered functional connectivity. We suggest that mismatch processing across large-scale networks may serve as a promising biomarker capturing several core impairments in schizophrenia.

Acknowledgements

The authors thank the Brain Imaging Facility of the IZKF Aachen, Bruno de Masiero, Roman Scharrer and Jan-Gerrit Richter from the RWTH Aachen Institute of Technical Acoustics as well as Cordula Kemper, Maria Peters, Juliane Brieger, Xenia Kobeleva and Hannes Schwenke from the RWTH Aachen University Hospital for their excellent technical support.

Funding

This research was supported by grants of the Medical Faculty of the RWTH Aachen University (START; 121/11 and 143/13) and the German Research Foundation (DFG; MA 2631/6-1, IRTG 1328).

References

Baldeweg T, Klugman A, Gruzelier JH, Hirsch SR. Impairment in frontal but not temporal components of mismatch negativity in schizophrenia. Int J Psychophysiol 2002; 43: 111–22.

Barbas H, Ghashghaei H, Dombrowski SM, Rempel-Clower NL. Medial prefrontal cortices are unified by common connections with superior temporal cortices and distinguished by input from memory-related areas in the rhesus monkey. J Comp Neurol 1999; 410: 343–67.

Barch DM, Ceaser A. Cognition in schizophrenia: core psychological and neural mechanisms. Trends Cogn Sci 2012; 16: 27–34.

Belger A, Yucel GH, Donkers F. In search of psychosis biomarkers in high-risk populations: is the mismatch negativity the one we've been waiting for? Biol Psychiatry 2012; 71: 94.

Benson PJ, Beedie SA, Shephard E, Giegling I, Rujescu D, St Clair D. Simple viewing tests can detect eye movement abnormalities that distinguish schizophrenia cases from controls with exceptional accuracy. Biol Psychiatry 2012; 72: 716–24.

Bishop CM. Pattern recognition and machine learning. New York: Springer-Verlag; 2006.

Catts SV, Shelley AM, Ward PB, Liebert B, Mc Conaghy N, Andrews S, et al. Brain potential evidence for an auditory sensory memory deficit in schizophrenia. Am J Psychiatry 1995; 152: 213–9.

Clark L, Bechara A, Damasio H, Aitken MRF, Sahakian BJ, Robbins TW. Differential effects of insular and ventromedial prefrontal cortex lesions on risky decision-making. Brain 2008; 131: 1311–22.

Corbetta M, Shulman GL. Control of goal-directed and stimulus-driven attention in the brain. Nature Rev Neurosci 2002; 3: 201–15.

Dinkel PJ, Willmes K, Krinzinger H, Konrad K, Koten JW Jr. Diagnosing developmental dyscalculia on the basis of reliable single case FMRI methods: promises and limitations. PLoS One 2013; 8: e83722.

Demirci O, Clark VP, Calhoun VD. A projection pursuit algorithm to classify individuals using fMRI data: application to schizophrenia. Neuroimage 2008; 39: 1774–82.

Fisher DJ, Grant B, Smith DM, Borracci G, Labelle A, Knott VJ. Nicotine and the hallucinating brain: effects on mismatch negativity (MMN) in schizophrenia. Psychiatry Res 2012; 196: 181–7.

Fletcher PC, Frith CD. Perceiving is believing: a Bayesian approach to explaining the positive symptoms of schizophrenia. Nat Rev Neurosci 2009; 10: 48–58.

Forman SD, Cohen JD, Fitzgerald M, Eddy WF, Mintun MA, Noll DC. Improved assessment of significant activation in functional magnetic resonance imaging (fMRI): use of a cluster-size threshold. Magn Reson Med 1995; 33: 636–47.

Fox MD, Snyder AZ, Vincent JL, Corbetta M, Van Essen DC, Raichle ME. The human brain is intrinsically organized into dynamic, anticorrelated functional networks. PNAS 2005; 102: 9673–8.

Friston KJ. Disconnection and cognitive dysmetria in schizophrenia. Am J Psychiatry 2005; 162: 429–32.

Friston KJ, Frith CD. Schizophrenia: a disconnection syndrome? Clin Neurosci 1995; 3: 89–97.

Friston KJ, Buechel C, Fink GR, Morris J, Rolls E, Dolan RJ. Psychophysiological and modulatory interactions in neuroimaging. Neuroimage 1997; 6: 218–29.

Garrido MI, Kilner JM, Stephan KE, Friston KJ. The mismatch negativity: a review of underlying mechanisms. Clin Neurophysiol 2009; 120: 453–63.

Harkrider AW, Hedrick MS. Acute effect of nicotine on auditory gating in smokers and non-smokers. Hear Res 2005; 202: 114–128.

Jardri R, Pouchet A, Pins D, Thomas P. Cortical activations during auditory verbal hallucinations in schizophrenia: a coordinate-based meta-analysis. Am J Psychiatry 2011; 168: 73–81.

Javitt DC. Sensory processing in schizophrenia: neither simple nor intact. Schizophr Bull 2009a; 35: 1059–64.

Javitt DC. When doors of perception close: bottom-up models of disrupted cognition in schizophrenia. Annu Rev Clin Psychol 2009b; 5: 249–75.

Javitt DC, Steinschneider M, Schroeder CE, Arezzo JC. Role of cortical N-methyl-D-aspartate receptors in auditory sensory memory and mismatch negativity generation: Implications for schizophrenia. Proc Natl Acad Sci USA 1996; 93: 11962–7.

Javitt DC, Grochowski S, Shelley AM, Ritter W. Impaired mismatch negativity (MMN) generation in schizophrenia as a function of stimulus deviance, probability, and interstimulus/interdeviant interval. Electroencephalogr Clin Neurophysiol 1998; 108: 143–53.

Kachel A, Biesiada J, Blachnik M, Duch W. (2010, January). Infosel++: Information based feature selection C++ library. In: Rutkowski L, Scherer R, Tadeusiewicz R, Zadeh LA, Zurada JM, editors. Artificial intelligence and soft computing Berlin Heidelberg: Springer-Verlag; 2010. p. 388–96.

Kähkönen S, Ahveninen J, Jääskeläinen IP, Kaakkola S, Näätänen R, Huttunen J, Pekkonen E. Effects of haloperidol on selective attention: a combined whole-head MEG and high-resolution EEG study. Neuropsychopharmacology 2001; 25: 498–504.

Kähkönen S, Ahveninen J, Pekkonen E, Kaakkola S, Huttunen J, Ilmoniemi RJ, Jääskeläinen IP. Dopamine modulates involuntary attention shifting and reorienting: an electromagnetic study. Clin Neurophysiol 2002; 113: 1894–902.

Kapur S. Psychosis as a state of aberrant salience: a framework linking biology, phenomenology, and pharmacology in schizophrenia. Am J Psychiatry 2003; 160: 13–23.

Kendall MG, Jean DG. Rank correlation methods. New York: Oxford University Press; 1990.

Kennerley SW, Walton ME, Behrens TEJ, Buckley MJ, Rushworth MFS. Optimal decision making and the anterior cingulate cortex. Nat Neurosci 2006; 9: 940–7.

Kincade JM, Abrams RA, Astafiev SV, Shulman GL, Corbetta M. An event-related functional magnetic resonance imaging study of voluntary and stimulus-driven orienting of attention. J Neurosci 2005; 25: 4593–604.

Kircher TT, Rapp A, Grodd W, Buchkremer G, Weiskopf N, Lutzenberger W, et al. Mismatch negativity responses in schizophrenia: a combined fMRI and whole-head MEG study. Am J Psychiatry 2004; 161: 294–304.

Knott V, Impey D, Philippe T, Smith D, Choueiry J, de la Salle S, et al. Modulation of auditory deviance detection by acute nicotine is baseline and deviant dependent in healthy nonsmokers: a mismatch negativity study. Hum Psychopharmacol 2014; 29: 446–58.

Leung S, Croft RJ, Baldeweg T, Nathan PJ. Acute dopamine D(1) and D(2) receptor stimulation does not modulate mismatch negativity (MMN) in healthy human subjects. Psychopharmacology 2007; 194: 443–51.

Leung S, Croft RJ, Guille V, Scholes K, O'Neill BV, Phan KL, et al. Acute dopamine and/or serotonin depletion does not modulate mismatch negativity (MMN) in healthy human participants. Psychopharmacology 2010; 208: 233–44.

Liddle PF, Friston KJ, Frith CD, Hirsch SR, Jones T, Frackowiak RS. Patterns of cerebral blood flow in schizophrenia. Br J Psychiatry 1992; 160: 179–86.

Lieder F, Stephan KE, Daunizeau J, Garrido MI, Friston KJ. A neurocomputational model of the mismatch negativity. PLoS Comput Biol 2013; 9: e1003288.

Mathiak K, Rapp A, Kircher TT, Grodd W, Hertrich I, Weiskopf N, et al. Mismatch responses to randomized gradient switching noise as reflected by fMRI and whole-head magnetoencephalography. Hum Brain Mapp 2002a; 16: 190–195.

Mathiak K, Hertrich I, Lutzenberger W, Ackermann H. Functional cerebral asymmetries of pitch processing during dichotic stimulus application: a whole-head magnetoencephalography study. Neuropsychologia 2002b; 40: 585–593.

Menon V. Large-scale brain networks and psychopathology: a unifying triple network model. Trends Cogn Sci 2011; 15: 483–506.

Murray GK, Corlett PR, Clark L, Pessiglione M, Blackwell AD, Honey G, et al. Substantia nigra/ventral tegmental reward prediction error disruption in psychosis. Mol Psychiatry 2008; 13: 239–76.

Näätänen R. The mismatch negativity: a powerful tool for cognitive neuroscience. Ear Hear 1995; 16: 6–18.

Näätänen R, Pakarinen S, Rinne T, Takegata R. The Mismatch negativity (MMN): towards the optimal paradigm. Clin Neurophysiol 2004; 115: 140–4.

Palaniyappan L, Liddle PF. Does the salience network play a cardinal role in psychosis? An emerging hypothesis of insular dysfunction. J Psychiatry Neurosci 2012; 37: 17–27.

Palaniyappan L, Mallikarjun P, Joseph V, White TP, Liddle PF. Reality distortion is related to the structure of the salience network in schizophrenia. Psychological Medicine 2011; 41: 1701–8.

Park HJ, Kwon JS, Youn T, Pae JS, Kim JJ, Kim MS, et al. Statistical parametric mapping of LORETA using high density EEG and individual MRI: application to mismatch negativities in schizophrenia. Hum Brain Mapp 2002; 17: 168–78.

Pekkonen E, Hirvonen J, Jaaskelainen IP, Kaakkola S, Huttunen . Auditory sensory memory and the cholinergic system: Implications for Alzheimer's disease. Neuroimage 2001; 14: 376–82.

Pekkonen E, Hirvonen J, Ahveninen J, Kähkönen S, Kaakkola S, Huttunen J, et al. Memory-based comparison process not attenuated by haloperidol: a combined MEG and EEG study. Neuroreport 2002; 13: 177–81.

Pekkonen E, Jääskeläinen IP, Kaakkola S, Ahveninen J. Cholinergic modulation of preattentive auditory processing in aging. Neuroimage 2005; 27: 387–92.

Potkin SG, Alva G, Fleming K, Anand R, Keator D, Carreon D, et al. A PET study of the pathophysiology of negative symptoms in schizophrenia. Am J Psychiatry 2002; 159: 227–37.

Preuschoff K, Quartz SR, Bossaerts P. Human insula activation reflects risk prediction errors as well as risk. J Neurosci 2008; 28: 2745–52.

Sato Y, Yabe H, Todd J, Michie P, Shinozaki N, Sutoh T, et al. Impairment in activation of a frontal attention-switch mechanism in schizophrenic patients. Biol Psychol 2003; 62: 49–63.

Schall U, Johnston P, Todd J, Ward PB, Michie PT. Functional neuroanatomy of auditory mismatch processing: an event-related fMRI study of duration-deviant oddballs. Neuroimage 2003; 20: 729–36.

Schmidt A, Bachmann R, Kometer M, Csomor PA, Stephan KE, Seifritz E, et al. Mismatch negativity encoding of prediction errors predicts S-ketamine-induced cognitive impairments. Neuropsychopharmacology 2012; 37: 865–75.

Schock L, Dyck M, Demenescu LR, Edgar JC, Hertrich I, Sturm W, et al. Mood modulates auditory laterality of hemodynamic mismatch responses during dichotic listening. PLoS One 2012; 7: e31936.

Schock L, Bhavsar S, Demenescu LR, Sturm W, Mathiak K. Does valence in the visual domain influence the spatial attention after auditory deviants? Exploratory data. Front Behav Neurosci 2013; 7: 6.

Seeley WW, Menon V, Schatzberg AF, Keller J, Glover GH, Kenna H, et al. Dissociable intrinsic connectivity networks for salience processing and executive control. J Neurosci 2007; 27: 2349–56.

Shelley AM, Silipo G, Javitt DC. Diminished responsiveness of ERPs in schizophrenic subjects to changes in auditory stimulation parameters: implications for theories of cortical dysfunction. Schizophr Res 1999; 37: 65–79.

Shen H, Wang L, Liu Y, Hu D. Discriminative analysis of resting-state functional connectivity patterns of schizophrenia using low dimensional embedding of fMRI. Neuroimage 2010; 49: 3110–21.

Siegel C, Waldo M, Mizner G, Adler LE, Freedman R. Deficits in sensory gating in schizophrenic patients and their relatives: evidence obtained with auditory evoked responses. Arch Gen Psychiatry 1984; 41: 607–12.

Stephan KE, Baldeweg T, Friston KJ. Synaptic plasticity and dysconnection in schizophrenia. Biol Psychiatry 2006; 59: 929–39.

Takahashi H, Rissling AJ, Pascual-Marqui R, Kirihara K, Pela M, Sprock J, et al. Neural substrates of normal and impaired preattentive sensory discrimination in large cohorts of nonpsychiatric subjects and schizophrenia patients as indexed by MMN and P3a change detection response. Neuroimage 2012; 66: 594–603.

Tang Y, Wang L, Cao F, Tan L. Identify schizophrenia using resting-state functional connectivity: an exploratory research and analysis. Biomed Eng Online 2012; 11: 50.

Tervaniemi M, Schröger E, Saher M, Näätänen R. Effects of spectral complexity and sound duration on automatic complex-sound pitch processing in humans - a mismatch negativity study. Neurosci Lett 2000; 290: 66–70.

Thönnessen H, Zvyagintsev M, Harke KC, Boers F, Dammers J, Norra C, et al. Optimized mismatch negativity paradigm reflects deficits in schizophrenia patients. A combined EEG and MEG study. Biol Psychol 2008; 77: 205–16.

Todd J, Michie PT, Schall U, Ward PB, Catts SV. Mismatch negativity (MMN) reduction in schizophrenia – impaired prediction error generation, estimation or salience? Int J Psychophysiol 2012; 83: 222–31.

Tombu M, Jolicoeur P. A central capacity sharing model of dual-task performance. J Exp Psychol Hum Percept Perform 2003; 29: 3–18.

Tzourio-Mazoyer N, Landeau B, Papathanassiou D, Crivello F, Etard O, Delcroix N, et al. Automated anatomical labeling of activations in SPM using a macroscopic anatomical parcellation of the MNI MRI single-subject brain. Neuroimage 2002; 15: 273–89.

Umbricht D, Koller R, Vollenweider FX, Schmid L. Mismatch negativity predicts psychotic experiences induced by NMDA receptor antagonist in healthy volunteers. Biol Psychiatry 2002; 51: 400–6.

Waberski TD, Kreitschmann-Andermahr I, Kawohl W, Darvas F, Ryang Y, Gobbele R, Buchner H. Spatio-temporal source imaging reveals subcomponents of the human auditory mismatch negativity in the cingulum and right inferior temporal gyrus. Neurosci Lett 2001; 308: 107–10.

Wang GJ, Volkow ND, Fowler JS, Ding YS, Logan J, Gatley SJ, et al. Comparison of two PET radioligands for imaging extrastriatal dopamine transporters in human brain. Life Sci 1995; 57: PL187–91.

White TP, Joseph V, Francis ST, Liddle PF. Aberrant salience network (bilateral insula and anterior cingulate cortex) connectivity during information processing in schizophrenia. Schizophr Res 2010; 123: 105–15.

Wible CG, Kubicki M, Yoo S-S, Kacher DF, Salisbury DF, Anderson MC, et al. A functional magnetic resonance imaging study of auditory mismatch in schizophrenia. Am J Psychiatry 2001; 158: 938–43.

Wienberg M, Glenthoj BY, Jensen KS, Oranje B. A single high dose of escitalopram increases mismatch negativity without affecting processing negativity or P300 amplitude in healthy volunteers. J Psychomarmacol 2010; 24: 1183–92.

Winkler I, Karmos G, Näätänen R. Adaptive modeling of the unattended acoustic environment reflected in the mismatch negativity event-related potential. Brain Res 1996; 742: 239–52.

Wolkin A, Sanfilipo M, Wolf AP, Angrist B, Brodie JD, Rotrosen J. Negative symptoms and hypofrontality in chronic schizophrenia. Arch Gen Psychiatry 1992; 49: 959–65.

Woodward ND, Zald DH, Ding Z, Ricardi P, Ansari MS, Baldwin RM, et al. Cerebral morphology and dopamine D2/D3 receptor distribution in humans: a combined [18F]fallypride and voxel-based morphometry study. Neuroimage 2009; 46: 31–8.

Zeng LL, Shen H, Liu L, Wang L, Li B, Fang P, et al. Identifying major depression using whole-brain functional connectivity: a multivariate pattern analysis. Brain 2012; 135: 1498–507.

Zvyagintsev M, Thönnessen H, Boers F, Dammers J, Mathiak K. An automatic procedure for analysis of electric and magnetic mismatch negativity based on brain mapping. J Neurosci Methods 2008; 168: 325–33.